TWMS J. App. and Eng. Math. V.15, N.5, 2025, pp. 1048-1062

ESTIMATING THE BOUND SET OF A CHAOTIC SYSTEM AND ITS APPLICATION IN CHAOS SYNCHRONIZATION

A. KHAN[1], S. ALI[1*], A. KHAN[1], §

Abstract. In this paper, we investigate the ultimate bound set for a chaotic system. Based on Lagrange multiplier method, an optimization problem has been done analytically to calculate a precise ultimate bound set of the chaotic system. Apart from that application of the bound set is also discussed and it can be used to study chaos synchronization. Synchronization has been realized between two identical chaotic systems via globally exponential approach. Resulting bound sets and synchronization are quantitatively tested to illustrate the effectiveness of the theoretical analysis.

Keywords: Lagrange multiplier, Ultimate bound set, Synchronization.

AMS Subject Classification: 34H10 , 34H15, 34D06 .

1. Introduction

E.N. Lorenz [1] introduced the idea of chaos using the weather model and obtained the first chaotic attractor-Lorenz system. The nonlinear systems exhibit complex behavior leads to chaos due to the sensitive dependence upon the initial conditions, which is known as butterfly's effect. The use of chaos theory is found in encrypted communication [2], biology [3], engineering technology [4, 5], many other fields and it has been studied thoroughly by researchers.

One interesting idea in chaos is to estimate the boundaries for the solution of chaotic systems to study the dynamical behaviour of a system more deeply. To find the ultimate bound sets attractive sets for a dynamical system is a crucial task and it has important application such as controlling and synchronizing chaotic systems, Hausdorff dimension, and identifying hidden attractors [6, 7, 8, 9, 10]. Under certain conditions, if one can able to determine an ultimate bound set (UBS) for a chaotic dynamical system, then it ensure that absence of periodic solutions, quasi-periodic solutions and equilibrium points outside the UBS of the system. In 1987, Leonov et al. [8] studied two bounds—a spherical bound and a cylindrical bound — for the globally attractive and positive invariant

[1] Department of Mathematics, Jamia Millia Islamia, New Delhi, India.
e-mail: akhan12@jmi.ac.in; ORCID: https://orcid.org/0009-0009-5317-6855.
e-mail: alishadabmath@gmail.com; ORCID: https://orcid.org/0009-0008-4938-9156.
e-mail: akhan2@jmi.ac.in; ORCID: https://orcid.org/0000-0003-3783-188X.
∗ Corresponding author.
§ Manuscript received: February 25, 2024; accepted: August 29, 2024.

sets of the Lorenz system. Li et al. [11] have analyzed the ultimate bound set for hyperchaotic Lorenz-Haken system. By applying dimension reduction method, Wang et al. [12] obtained explicit bound sets for the hyperchaotic Lorenz-Stenflo system. Using the extremum principle of function and generalised Lyapunov function theory, Nik et al. [13] obtained ultimate bound sets for the hyperchaotic system. After constructing a suitable Lyapunov function, boundedness of the solutions of Chen system [14] and Lü system [15] has been discussed also. Recently, Lei et al. [16] have spotlighted the complete inaccuracy of the results regarding estimating the ultimate bound set [17]. Wang and Dong [18] then looked into the boundedness of the system once again by considering an appropriate Lyapunov function and demonstrated that the solutions of system are globally bounded in the designated areas. To get the ultimate bound estimation of any existing chaotic and hyperchaotic systems, the common approach can be followed for optimization methodology and Lyapunov function. However, the search for Lyapunov functions and ultimate bound sets corresponding to hyperchaotic attractors is much more difficult than the chaotic attractor. Consequently, the ultimate bound estimation for hyperchaotic systems can be typically observed as an optimization problem. Based on these, Wang et al. [19] developed a unified approach for estimating the ultimate bound for a certain class of high-dimensional quadratic autonomous dynamical systems and studied it in two chaotic systems and a hyperchaotic system, respectively. Using this unified approach, authors estimated the bounded sets of various hyper-chaotic and chaotic systems [10, 20]. Moreover, researchers are interested to study the estimation of the bound set in case of fractional-order chaotic system [21, 22, 23]. Studies related to ultimate bound estimation has been the subject of extensive interest. These deliberations have been done in case of chaotic systems which is the key component of present scenario.

The technique for controlling chaos is Predictive control and synchronization [24]. The phenomenon of having many chaotic systems—whether identical or not—following the same path is known as chaos synchronization. In other words, the behavior of one system merges with the behaviour of another, forcing them to synchronize in a way that triggers the states of both systems reaching asymptotically to each other. Carroll and Pecora [25] initially proposed the concept of synchronization in order to design the appropriate controllers to synchronize two chaotic systems with distinct initial conditions. There are variety of control strategies, such as active control, sliding mode control, adaptive control, and others. Complete synchronization, anti-synchronization, compound synchronization, difference synchronization and others have been developed to control the chaotic behaviour of systems [26, 27, 28, 29]. Among all the control techniques for chaos synchronization, linear feedback control is the most common, simple and easy to bring in practice. Many authors have used the linear feedback control approach to synchronize and control chaos in various chaotic and hyper chaotic systems such as Rössler system [30], Lorenz system [31] and other nonlinear systems [32]. These control techniques are too appealing and have been widely used due to their simplicity in configuration and implementation. Linear feedback synchronization approach has been used to achieve the globally exponentially synchronization [33, 34] and lyapunov stability theory ensure the global stability of the nonlinear systems. The main features of the paper are as follows:

–This paper focuses on two aspects: First is to estimate the ultimate bound set of a chaotic system, and secondly the investigation of synchronization between two identical systems for chaotic systems with the idea of bound set.

–To obtain ultimate bound set of the chaotic system, a combination of Lyapunov stability theory and Lagrange optimization method have been applied.

–Globally exponential synchronization has been achieved between two identical chaotic

systems.
–Numerical simulations have been carried out to demonstrate the effectiveness of this technique by using the concept of determined ultimate bound set.
–Comparison analysis has been done with relative existing literature.

This article has been organised as follows: Section 2 discusses the dynamics of a chaotic system. Section 3 deals with method description and estimation of ultimate bound set of the system. Section 4 contains globally exponential synchronization scheme via linear feedback control. Section 5 provides the numerical simulations. Section 6 includes the comparative analysis. Conclusion is drawn in section 7.

2. Dynamics of 3D system

Consider the 3D chaotic system [35] as follows:

$$\begin{cases} \dot{w}_1 = \frac{1}{3}w_2w_3 - \alpha w_1 + \frac{1}{\sqrt{6}}w_3, \\ \dot{w}_2 = -w_1w_3 + \beta w_2, \\ \dot{w}_3 = w_1w_2 - \sqrt{6}w_1 - \gamma w_3, \end{cases} \tag{1}$$

where α, β and γ are the parameters and w_i for $i = 1, 2, 3$, are state variables of the system (1). For $\alpha = 0.400$, $\beta = 0.175$, and $\gamma = 0.400$, Lyapunov exponents of the system (1) at $t = 300$ with initial conditions $(1, 1.5, 2.5)$ are $\lambda_1 = 0.1501$, $\lambda_2 = 0.0050$, and $\lambda_3 = -0.7802$. In Fig.1, we observe that one of the three lyapunov exponents value is positive, one lyapunov exponent is near to zero, while the remaining one lyapunov exponent is negative, which ensure the chaotic behaviour of the system. Chaotic attractors can be seen in Fig.2.

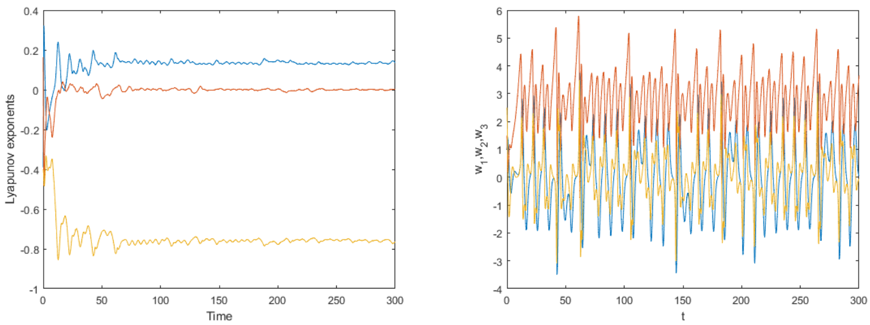

(A) (B)

Figure 1. **(A)** Lyapunov exponents; **(B)** State trajectories of chaotic system (1).

3. Boundedness of the chaotic system

To compute the ultimate bound set of the chaotic system, first we describe the technique before addressing the optimization issue and its analytical solution.

3.1. **Method description.** Assuming $W = (w_1, w_2, ..., w_n)^T$ to be the solution of the following autonomous system:

$$\frac{dW}{dt} = f(W), \tag{2}$$

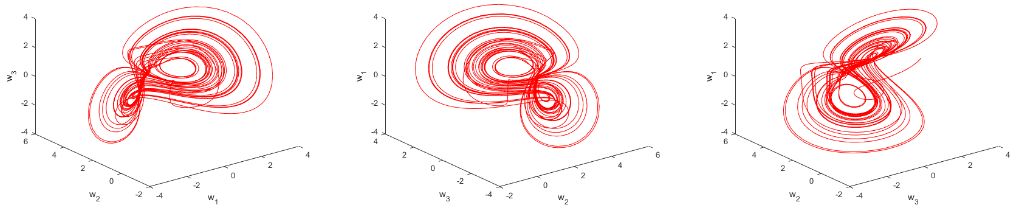

(A) (B) (C)

FIGURE 2. **(A)**, **(B)**, **(C)** show chaotic attractors of the chaotic system (1) for parameters $\alpha = 0.400$, $\beta = 0.175$,$\gamma = 0.400$ with initial conditions $(1, 1.5, 2.5)$.

where $f : \mathbb{R}^n \to \mathbb{R}^3$. Let $W_0 = W(t_0, t_0, W_0)$ is the initial value of $W(t, t_0, W_0)$, and $\mho \subset \mathbb{R}^n$ is the compact set. The distance between $W(t, t_0, W_0)$ and $\mho$ described η is given as,

$$\eta(W(t, t_0, W_0), \mho) = \inf_{Y \in \mho} ||W(t, t_0, W_0) - Y||.$$

Suppose for each $\chi > 0$, $\mho_\chi = \{W | \eta(W, \mho) < \chi\}$, then we have $\mho \subset \mho_\chi$.

Definition 3.1. *Assume that there is a compact set $\mho \in \mathbb{R}^n$ fulfilling the following criterion* [19]*:*

$$\lim_{t \to \infty} \eta(W(t), \mho) = 0, \qquad \forall\ W_0 \in \mathbb{R}^n / \mho, \tag{3}$$

i.e., for each $\chi > 0$, there exists $T > t_0$, such that $W(t, t_0, W_0) \in \mho_\chi$ for all $t \geq T$. The set $\mho_\chi$ is said to be an ultimate bound set (USB) of system (2). If, for any $W_0 \in \mho$ and for all $t \geq t_0$, $W(t, t_0, W_0) \in \mho$, then $\mho$ is called the positively invariant set for system (2).

To determine the bound set of a dynamical system, let us rewrite the system (2) as:

$$\dot{W} = AW + \sum_{i=1}^{n} w_i H_i W + U, \tag{4}$$

where $W = (w_1, w_2, ..., w_n)^T \in \mathbb{R}^n$ are system state vectors. Also, $A \in \mathbb{R}^{n \times n}$, $U \in \mathbb{R}^n$, and $H_i = (h^i_{jk})_{n \times n} \in \mathbb{R}^{n \times n}$ with every element of H_i satisfying $h^i_{jk} = h^j_{ik}$, for all $i, j, k = 1, 2, ..., n$.

The quadratic function $\mathcal{V}$ is defined as follows:

$$\mathcal{V}(W) = (W + \psi)^T M (W + \psi), \tag{5}$$

where $M = M^T = (m_{ij})_{n \times n}$ for all $i, j = 1, 2, ..., n$ is a symmetric matrix and $\psi = (\psi_1, \psi_2, ..., \psi_n) \in \mathbb{R}^{n \times n}$ are real parameters to be calculated. Taking the derivative of (5), we get,

$$\dot{\mathcal{V}}(W) = \dot{W}^T M (W + \psi) + (W + \psi)^T M \dot{W}, \tag{6}$$

$$\begin{aligned} \dot{\mathcal{V}}(W) &= W^T [A^T M + MA + 2(H_1^T M\psi, H_2^T M\psi, ..., H_n^T M\psi)^T] W \\ &\quad + \sum_{i=1}^{n} w_i W^T (H_i^T M + M H_i) + 2(\psi^T MA + U^T M) W + 2U^T M\psi. \end{aligned} \tag{7}$$

Denoting $\quad Q = A^T M + MA + 2(H_1^T M\psi, H_2^T M\psi, ..., H_n^T M\psi)^T$
and $G = 2(\psi^T MA + U^T M)$.

One gets,

$$\dot{\mathcal{V}}(W) = W^T Q W + \sum_{i=1}^{n} w_i W^T (H_i^T M + M H_i) W + G W + 2U^T M \psi. \tag{8}$$

Theorem 3.1. [19] *Suppose that $M > 0$ is a positive definite symmetric matrix and $\psi \in \mathbb{R}^n$ is a vector, such that*

$$Q = A^T M + M A + 2(H_1^T M \psi, H_2^T M \psi, ..., H_n^T M \psi)^T < 0, \tag{9}$$

and for any $W = (w_1, w_2, ..., w_n)^T \in \mathbb{R}^n$

$$\sum_{i=1}^{n} w_i W^T (H_i^T M + M H_i) W = 0, \tag{10}$$

then system (4) is bounded and its ultimate bound set is defined as follows:

$$\mho = \{W \in \mathbb{R}^n : (W + \psi)^T M (W + \psi) \leq J\}, \tag{11}$$

where J is a real value to be determined by following optimization problem :

$$\begin{aligned} &\textit{maximize } \ (W + \psi)^T M (W + \psi) \\ &\textit{subject to } \ W^T Q W + 2(\psi^T M A + U^T M) W + 2U^T M \psi = 0. \end{aligned} \tag{12}$$

3.2. **Estimation of the ultimate bound set for the chaotic system.** Description of the methodology to compute the bound set of the satellite chaotic system with help of Theorem 3.1 has been discussed in part. For that we rewrite the system (1) in the form of equation (4) as follows:

$$\dot{W} = AW + \sum_{i=1}^{3} w_i H_i W + U, \tag{13}$$

where

$$A = \begin{pmatrix} -\alpha & 0 & \frac{1}{\sqrt{6}} \\ 0 & \beta & 0 \\ -\sqrt{6} & 0 & -\gamma \end{pmatrix}, \quad H_1 = \begin{pmatrix} 0 & 0 & 0 \\ 0 & 0 & -\frac{1}{2} \\ 0 & \frac{1}{2} & 0 \end{pmatrix}, \quad H_2 = \begin{pmatrix} 0 & 0 & \frac{1}{6} \\ 0 & 0 & 0 \\ \frac{1}{2} & 0 & 0 \end{pmatrix},$$

$$H_3 = \begin{pmatrix} 0 & \frac{1}{6} & 0 \\ -\frac{1}{2} & 0 & 0 \\ 0 & 0 & 0 \end{pmatrix}, \quad \text{and} \quad U = \begin{pmatrix} 0 \\ 0 \\ 0 \end{pmatrix}.$$

Let $M = M^T = (m_{ij})_{3\times 3}$, $i, j = 1, 2, 3$. From the equation (10), we have

$$\sum_{i=1}^{3} w_i W^T (H_i^T M + M H_i) W = 0, \tag{14}$$

holds for any $w_i \in \mathbb{R}$, $i = 1, 2, 3$. Therefore,

$$\begin{aligned} &m_{13} w_1^2 w_2 m_{21}\left(-w_1^2 w_3 + \frac{w_2^2 w_3}{3}\right) + m_{12}(w_1^2 w_3 + w_2^2 w_3) + m_{31}\left(w_1^2 w_2 + \frac{w_2 w_3^2}{3}\right) \\ &+ m_{13}\left(w_1^2 w_2 + \frac{w_2 w_3^2}{3}\right) + m_{32}\left(w_1 w_2^2 - w_1 w_3^2\right) + m_{23}\left(w_1 w_2^2 - w_1 w_3^2\right) \\ &+ \left(m_{33} - m_{22} + m_{33} + \frac{m_{11}}{3} + \frac{m_{11}}{3} - m_{22}\right) w_1 w_2 w_3 = 0. \end{aligned} \tag{15}$$

Let $m_{13} = m_{21} = m_{32} = 0$, $m_{33} - m_{22} + m_{33} + \frac{m_{11}}{3} + \frac{m_{11}}{3} - m_{22} = 0$. Corresponding to these calculation the matrix M becomes,

$$M = \begin{pmatrix} m_{11} & 0 & 0 \\ 0 & m_{33} + \frac{m_{11}}{3} & 0 \\ 0 & 0 & m_{33} \end{pmatrix},$$

and one can also obtain,

$$Q = \begin{pmatrix} -2\alpha m_{11} & m_{33}\psi_3 & \frac{m_{11}}{\sqrt{6}} - m_{33}\sqrt{6} - \Big(m_{33} + \frac{m_{11}}{3}\Big)\psi_2 \\ m_{33}\psi_3 & 2\beta\Big(m_{33} + \frac{m_{11}}{3}\Big) & \frac{m_{11}}{3}\psi_1 \\ \frac{m_{11}}{\sqrt{6}} - m_{33}\sqrt{6} - \Big(m_{33} + \frac{m_{11}}{3}\Big)\psi_2 & \frac{m_{11}}{3}\psi_1 & -2\gamma m_{33} \end{pmatrix}.$$

For simplification, we choose $\psi = (\psi_1, \psi_2, \psi_3) = \Big(0, \frac{-1}{m_{33} + \frac{m_{11}}{3}}, 0\Big)$,

$$Q = \begin{pmatrix} -2\alpha m_{11} & 0 & \Big(\frac{m_{11}}{\sqrt{6}} - m_{33}\sqrt{6}\Big) + 1 \\ 0 & 2\beta\Big(m_{33} + \frac{m_{11}}{3}\Big) & 0 \\ \Big(\frac{m_{11}}{\sqrt{6}} - m_{33}\sqrt{6}\Big) + 1 & 0 & -2\gamma m_{33} \end{pmatrix}.$$

Expressing $\Big(\frac{m_{11}}{\sqrt{6}} - m_{33}\sqrt{6}\Big) = \tau_1$ and $\Big(m_{33} + \frac{m_{11}}{3}\Big) = \tau_2$, then

$$Q = \begin{pmatrix} -2\alpha m_{11} & 0 & \tau_1 + 1 \\ 0 & 2\beta\tau_2 & 0 \\ \tau_1 + 1 & 0 & -2\gamma m_{33} \end{pmatrix}.$$

Subsequently, we get

$$\mathcal{V}(W) = (W + \psi)^T M (W + \psi), \tag{16}$$

$$\mathcal{V}(W) = m_{11}w_1^2 + \tau_2\Big(w_2 - \frac{1}{\tau_2}\Big)^2 + m_{33}w_3^2. \tag{17}$$

$\dot{\mathcal{V}}(W) = 0$ gives

$$-\alpha m_{11}w_1^2 + \beta\tau_2 w_2^2 - \gamma m_{33}w_3^2 + (\tau_1 + 1)w_1w_3 - \beta w_2 = 0. \tag{18}$$

Since, $\dot{\mathcal{V}}(W)$ describes an ellipsoidal surface. Therefore in case of $\dot{\mathcal{V}}(W) = 0$, $\mathcal{V}(W)$ obtains its maximum value on the ellipsoidal surface. Thus, the problem has an optimal solution. Let us assume that J be the optimal solution of the problem (12). Now,

$$\mho = \Big\{W(t) = (w_1, w_2, w_3) \in \mathbb{R}^3 : m_{11}w_1^2 + \tau_2\Big(w_2 - \frac{1}{\tau_2}\Big)^2 + m_{33}w_3^2 \le J\Big\} \tag{19}$$

is a compact set for any $M > 0$. We require to show that

$$\lim_{t\to\infty} \eta(W, \mho) = 0.$$

If $\lim_{t\to\infty} \eta(W, \mho) \neq 0$, then the solutions of the system (13) will remain in $\mathbb{R}^3/\mho$ forever and $\dot{\mathcal{V}}(W) < 0$. Hence, $\mathcal{V}(W(t))$ uniformly deceases in $\mathbb{R}^3/\mho$, and we have,

$$\lim_{t\to\infty} \mathcal{V}(W(t)) = \mathcal{V}^* > J.$$

Let $B = \{W(t) : \mathcal{V}^* \leq \mathcal{V}(W(t)) \leq \mathcal{V}(W(t_0))\}$, where t_0 represents the starting time, and $B_1 = \inf\{-\dot{\mathcal{V}}(W(t)) : W \in B\}$. Clearly, $B_1 > 0$ and $\mathcal{V}^* > 0$ are the constants and $\dot{\mathcal{V}}(W(t)) \leq -B_1$ as $t \to \infty$. Thus, one can get, $0 \leq \mathcal{V}(W(t)) \leq \mathcal{V}(W(t_0)) - B_1(t-t_0)$ tends to $-\infty$. Consequently, we get

$$\lim_{t\to\infty} \eta(W, \mho) = 0.$$

This indicates that system (13) is bounded and $\mho$ is ultimate bound of the system (13).

Lemma 3.1. *Suppose that α, β, γ, m_{11}, m_{22} and m_{33} all are positive real values and*

$$\mho = \left\{W(t) \in \mathbb{R}^3 : m_{11}w_1^2 + \tau_2\left(w_2 - \frac{1}{\tau_2}\right)^2 + m_{33}w_3^2 \leq J\right\}. \tag{20}$$

Then, the system (13) has an ultimate bound set $\mho$, where

$$J = \frac{1}{\tau_2} = \frac{1}{m_{33} + \frac{m_{11}}{3}}, \qquad (\alpha, \beta, \gamma) \in E_3 \tag{21}$$

and,
$E_1 = \{(\alpha, \beta, \gamma) \in \mathbb{R}^{3^+} : \alpha > \gamma > 0\}$,
$E_2 = \{(\alpha, \beta, \gamma) \in \mathbb{R}^{3^+} : \gamma > \alpha > 0\}$,
$E_3 = \mathbb{R}^{3^+} \sim (E_1 \cup\ E_2)$.

Proof. In order to optimize, consider

$$\begin{aligned} &max\ \mathcal{V} = m_{11}w_1^2 + \tau_2\left(w_2 - \frac{1}{\tau_2}\right)^2 + m_{33}w_3^2, \\ &s.t\ -\alpha m_{11}w_1^2 + \beta\tau_2 w_2^2 - \gamma m_{33}w_3^2 + (\tau_1+1)w_1w_3 - \beta w_2 = 0. \end{aligned} \tag{22}$$

Expressing $\sqrt{m_{11}}w_1 = y_1$, $\sqrt{\tau_2}w_2 - \frac{1}{\sqrt{\tau_2}} = y_2$, $\sqrt{m_{33}}w_3 = y_3$. The above equations can be rewritten as follows:

$$\begin{aligned} &max\ \mathcal{V} = y_1^2 + y_2^2 + y_3^2 \\ &s.t\ \ -\alpha y_1^2 + \beta\left(y_2 + \frac{1}{\sqrt{\tau_2}}\right)^2 - \gamma y_3^2 + \frac{(\tau_1+1)y_1y_3}{\sqrt{m_{11}m_{33}}} - \frac{\beta}{\sqrt{\tau_2}}\left(y_2 + \frac{1}{\sqrt{\tau_2}}\right) = 0. \end{aligned} \tag{23}$$

Using the Lagrange method, Θ is defined as,

$$\Theta = y_1^2+y_2^2+y_3^2-\zeta\left[-\alpha y_1^2+\beta\left(y_2+\frac{1}{\sqrt{\tau_2}}\right)^2-\gamma y_3^2+\frac{(\tau_1+1)y_1y_3}{\sqrt{m_{11}m_{33}}}-\frac{\beta}{\sqrt{\tau_2}}\left(y_2+\frac{1}{\sqrt{\tau_2}}\right)\right]. \tag{24}$$

$$\begin{aligned} \frac{\partial\Theta}{\partial y_1} &= 2y_1 - \zeta\left[2\alpha y_1 - \frac{(\tau_1+1)y_3}{\sqrt{m_{11}m_{33}}}\right] = 0, \\ \frac{\partial\Theta}{\partial y_2} &= 2y_2 - \zeta\left[-2\beta\left(y_2 + \frac{1}{\tau_2}\right) + \frac{\beta}{\tau_2}\right] = 0, \\ \frac{\partial\Theta}{\partial y_3} &= 2y_3 - \zeta\left[2\gamma y_3 - \frac{(\tau_1+1)y_1}{\sqrt{m_{11}m_{33}}}\right] = 0, \\ \frac{\partial\Theta}{\partial\zeta} &= -\left[\alpha y_1^2 + \beta\left(y_2 + \frac{1}{\sqrt{\tau_2}}\right)^2 - \gamma y_3^2 + \frac{(\tau_1+1)y_1y_3}{\sqrt{m_{11}m_{33}}} - \frac{\beta}{\sqrt{\tau_2}}\left(y_2 + \frac{1}{\sqrt{\tau_2}}\right)\right] = 0. \end{aligned} \tag{25}$$

(i) If $\zeta = \frac{1}{\alpha}$ and $\alpha > \gamma > 0$, then we obtain

$$(y_1^\star, y_2^\star, y_3^\star) = \left(\pm i\frac{\beta}{2\sqrt{\tau_2}(\alpha+\beta)}\sqrt{\frac{(2\alpha+\beta)}{\alpha}}, \frac{-\beta}{2\sqrt{\tau_2}(\alpha+\beta)}, 0\right), \tag{26}$$

(ii) If $\zeta = \frac{1}{\gamma}$ and $\gamma > \alpha > 0$, then we obtain

$$(y_1^\star, y_2^\star, y_3^\star) = \left(0, \frac{-\beta}{2\sqrt{\tau_2}(\gamma+\beta)}, \pm i \frac{\beta}{2\sqrt{\tau_2}(\gamma+\beta)}\sqrt{\frac{(2\gamma+\beta)}{\gamma}}\right), \tag{27}$$

complex critical points are not to be considered.

(iii) $If \zeta \neq \frac{1}{\alpha}$ or $\left(\neq \frac{1}{\gamma}\right)$, then we obtain

$$(y_1^\star, y_2^\star, y_3^\star) = \left(0, -\frac{1}{\sqrt{\tau_2}}, 0\right). \tag{28}$$

Hence $\mathcal{V}_1 = \mathcal{V}_1(y_1^\star, y_2^\star, y_3^\star) = \frac{1}{\tau_2}$,
or $(y_1^\star, y_2^\star, y_3^\star) = (0, 0, 0)$, $\mathcal{V}_2 = \mathcal{V}_2(y_1^\star, y_2^\star, y_3^\star) = 0$.

Clearly, equation (23) represents the ellipsoidal surface, thus $\mathcal{V}$ shall have its minimum and maximum values. Let us assume that the minimal value of $\mathcal{V}$ is $\mathcal{V}_2 = 0$, and the maximum value is $\mathcal{V}_{max}$.

For simplicity,one can denote,
$E_1 = \{(\alpha, \beta, \gamma) \in \mathbb{R}^{3^+} : \alpha > \gamma > 0\}$,
$E_2 = \{(\alpha, \beta, \gamma) \in \mathbb{R}^{3^+} : \gamma > \alpha > 0\}$,
$E_3 = \mathbb{R}^{3^+} \sim (E_1 \cup \ E_2)$.
Hence, we obtain,

$$\mathcal{V}_{max} = \frac{1}{\tau_2} = \frac{1}{m_{33} + \frac{m_{11}}{3}}, \qquad (\alpha, \beta, \gamma) \in E_3, \tag{29}$$

and knowing that $\mathcal{V}_{max} = J$. This completes the proof. □

4. Synchronization via linear feedback control

In this section, we discuss the exponential synchronization of the chaotic system. This study is based on the conclusions of the calculation of ultimate bound set of the system (1). First, let us state the following lemma:

Lemma 4.1. *For any $\mu > 0$, w_1, $w_2 \in \mathbb{R}$, then the inequality $2w_1w_2 \leq \mu w_1^2 + \frac{1}{\mu}w_2^2$ holds.*

Consider the chaotic system (1) as master (drive) system, and the corresponding slave (response) system is defined as follows:

$$\begin{cases} \dot{z}_1 = \frac{1}{3}z_2z_3 - \alpha z_1 + \frac{1}{\sqrt{6}}z_3 + p_1, \\ \dot{z}_2 = -z_1z_3 + \beta z_2 + p_2, \\ \dot{z}_3 = z_1z_2 - \sqrt{6}z_1 - \gamma z_3 + p_3, \end{cases} \tag{30}$$

where z_1, z_2, z_3 are the states vectors of the system with parameters $\alpha = 0.400$, $\beta = 0.175$, $\gamma = 0.400$, and p_1, p_2, p_3 are the controllers to be designed to achieve the synchronization between master(drive) system (1) and slave(response) system (30). However, by using Theorem 3.1 one obtain,

$$\begin{cases} |w_1| \leq \sqrt{\frac{J}{m_{11}}} = \Delta_1, \\ |w_2| \leq \left|w_2 - \frac{1}{\tau_2}\right| + \frac{1}{\tau_2} = \sqrt{\frac{J}{\tau_2}} + \frac{1}{\tau_2} = \Delta_2, \\ |w_3| \leq \sqrt{\frac{J}{m_{33}}} = \Delta_3, \end{cases} \tag{31}$$

where J is defined in equation (21).

Theorem 4.1. *Consider the master system (1) and corresponding slave system (30). If we choose the controllers values as follows:*

$$p_1 = -k_1 e_1, p_2 = -k_2 e_2,\ p_3 = -k_3 e_3,$$

where $k_1 > \frac{\Delta_2}{3\sqrt{\sigma}} - 3\alpha - \frac{1}{\sqrt{6}\sqrt{\sigma}} - \frac{\Delta_3}{6\sqrt{\sigma}}$, $k_2 > \beta - \frac{\Delta_1}{4\sqrt{\sigma}} - \frac{\Delta_3\sqrt{\sigma}}{4}$, $k_3 > \Delta_2\sqrt{\sigma} - \frac{\Delta_1\sqrt{\sigma}}{2} - \frac{\sqrt{\sigma}}{2} - \gamma$, *and* $\sigma > 0$ *is real positive parameter. Then, the master (drive) system (1) and slave (response) system (30) are exponentially synchronized.*

Proof. We define the error system as,

$$e_1 = z_1 - w_1,\ \ e_2 = z_2 - w_2,\ \ and\ \ e_3 = z_3 - w_3. \tag{32}$$

Error dynamics becomes,

$$\begin{cases} \dot{e}_1 = \dot{z}_1 - \dot{w}_1, \\ \dot{e}_2 = \dot{z}_2 - \dot{w}_2, \\ \dot{e}_3 = \dot{z}_3 - \dot{w}_3. \end{cases} \tag{33}$$

It follows that,

$$\begin{cases} \dot{e}_1 = -\alpha e_1 + \frac{1}{\sqrt{6}} e_3 + \frac{1}{3} w_3 e_2 + \frac{1}{3} e_2 e_3 + p_1, \\ \dot{e}_2 = \beta e_2 - w_1 e_3 - w_3 e_1 - e_1 e_3 + p_2, \\ \dot{e}_3 = -\sqrt{6} e_1 - \gamma e_3 + w_1 e_2 + w_2 e_1 + e_1 e_2 + p_3. \end{cases} \tag{34}$$

Take the Lyapunov function as follows:

$$\begin{aligned} \nu(e_1, e_2, e_3) &= \frac{3}{2}\sigma e_1^2 + \sigma e_2^2 + \frac{1}{2}\sigma e_3^2. \\ \dot{\nu}(e_1, e_2, e_3) &= 3\sigma e_1 \dot{e_1} + \sigma e_2 \dot{e_2} + \sigma e_3 \dot{e}_3, \end{aligned} \tag{35}$$

Therefore,

$$\begin{aligned} \dot{\nu}(e) = 3\sigma e_1 &\bigg(-\alpha e_1 + \frac{1}{\sqrt{6}} e_3 + \frac{1}{3} w_3 e_2 + \frac{1}{3} e_2 e_3 - k_1 e_1 \bigg) \\ &+ \sigma e_2 \bigg(\beta e_2 - w_1 e_3 - w_3 e_1 - e_1 e_3 - k_2 e_2 \bigg) \\ &+ \sigma e_3 \bigg(-\sqrt{6} e_1 - \gamma e_3 + w_1 e_2 + w_2 e_1 + e_1 e_2 - k_3 e_3 \bigg), \end{aligned} \tag{36}$$

$$\begin{aligned} \text{that is} \qquad \dot{\nu}(e) &= -3(\alpha + k_1)\sigma e_1^2 + 2(\beta - k_2)\sigma e_2^2 - (\gamma + k_3)\sigma e_3^2 \\ &- \left(\sqrt{6} - \frac{3}{\sqrt{6}} \right) \sigma e_1 e_3 + 2\sigma e_1 e_3 w_2 - \sigma e_2 e_3 w_1 - \sigma e_1 e_2 w_3. \end{aligned} \tag{37}$$

By using Lemma 4.1, we get

$$\begin{cases} \sigma e_1 e_3 \leq \sigma^{\frac{1}{4}} |e_1| \sigma^{\frac{3}{4}} |e_3| \leq \frac{\sqrt{\sigma}}{2} e_1^2 + \frac{\sigma\sqrt{\sigma}}{2} e_3^2, \\ \sigma e_1 e_3 w_2 \leq \sigma |e_1||e_3| \Delta_2 \leq \frac{\Delta_2}{2} \sqrt{\sigma} e_1^2 + \frac{\Delta_2}{2} \sigma \sqrt{\sigma} e_3^2, \\ \sigma e_2 e_3 w_1 \leq \sigma |e_1||e_3| \Delta_1 \leq \frac{\Delta_1}{2} \sqrt{\sigma} e_2^2 + \frac{\Delta_1}{2} \sigma \sqrt{\sigma} e_3^2, \\ \sigma e_1 e_2 w_3 \leq \sigma |e_1||e_3| \Delta_1 \leq \frac{\Delta_1}{2} \sqrt{\sigma} e_2^2 + \frac{\Delta_1}{2} \sigma \sqrt{\sigma} e_3^2. \end{cases} \tag{38}$$

Then from equation (36) and (38), we have

$$\begin{aligned}
\dot{\nu} &\leq -3(\alpha + k_1)\sigma e_1^2 + 2(\beta - k_2)\sigma e_2^2 - (\gamma + k_3)\sigma e_3^2 \\
&\quad - \frac{3}{\sqrt{6}}\left(\frac{\sqrt{\sigma}}{2}e_1^2 + \frac{\sigma\sqrt{\sigma}}{2}e_3^2\right) + \left(\frac{\Delta_2}{2}\sqrt{\sigma}e_1^2 + \frac{\Delta_2}{2}\sigma\sqrt{\sigma}e_3^2\right) \\
&\quad - \left(\frac{\Delta_1}{2}\sqrt{\sigma}e_2^2 + \frac{\Delta_1}{2}\sigma\sqrt{\sigma}e_3^2\right).
\end{aligned}$$

This implies that

$$\begin{aligned}
\dot{\nu} &\leq -\left(3\alpha\sigma + 3k_1\sigma + \frac{3}{\sqrt{6}}\sqrt{\sigma} - \Delta_2\sqrt{\sigma} + \frac{\Delta_3}{2}\sqrt{\sigma}\right)e_1^2 \\
&\quad - \left(2k_2\sigma - 2\beta\sigma + \frac{\Delta_1}{2}\sqrt{\sigma} + \frac{\Delta_3}{2}\sigma\sqrt{\sigma}\right)e_2^2 \\
&\quad - \left(\gamma\sigma + k_3\sigma + \frac{3}{\sqrt{6}}\sigma\sqrt{\sigma} + \frac{\Delta_1}{2}\sigma\sqrt{\sigma} - \Delta_2\sigma\sqrt{\sigma}\right)e_3^2.
\end{aligned} \tag{39}$$

Set

$$\begin{cases}
3\alpha\sigma + 3k_1\sigma + \frac{3}{\sqrt{6}}\sqrt{\sigma} - \Delta_2\sqrt{\sigma} + \frac{\Delta_3}{2}\sqrt{\sigma} = \hat{\alpha}_1 > 0, \\
2k_2\sigma - 2\beta\sigma + \frac{\Delta_1}{2}\sqrt{\sigma} + \frac{\Delta_3}{2}\sigma\sqrt{\sigma} = \hat{\alpha}_2 > 0, \\
\gamma\sigma + k_3\sigma + \frac{3}{\sqrt{6}}\sigma\sqrt{\sigma} + \frac{\Delta_1}{2}\sigma\sqrt{\sigma} - \Delta_2\sigma\sqrt{\sigma} = \hat{\alpha}_3 > 0, \\
\hat{\alpha} = \min\{\hat{\alpha}_1, \hat{\alpha}_2, \hat{\alpha}_3\} > 0.
\end{cases} \tag{40}$$

Then,

$$\begin{aligned}
\dot{\nu} &\leq \hat{\alpha}_1 e_1^2 - \hat{\alpha}_2 e_2^2 - \hat{\alpha}_3 e_3^2, \\
\dot{\nu} &\leq -\hat{\alpha}\nu.
\end{aligned}$$

Hence, $\nu(t) \leq \nu(t_0)e^{-\hat{\alpha}(t-t_0)}$. It shows that the master (drive) system (1) and slave (response) system (30) are synchronized globally exponentially, as shown in Fig.7. □

5. Numerical Simulations

In this section, we discuss the numerical simulations to illustrate the validation of analytical method which is used to determine the ultimate bound of the chaotic system. Lyapunov exponents of system (1) at $t = 200$ for the parameter values $\alpha = 0.400$, $\beta = 0.175$, and $\gamma = 0.400$ as: $\lambda_1 = 0.1501$, $\lambda_2 = 0.0050$, and $\lambda_3 = -0.7802$. In Fig.1, we observe that one of the three Lyapunov exponents values is positive, one goes to zero, and one is negative, which is a necessary requirement for chaotic behaviour of the systems. It confirmed that the three-dimensional satellite system is chaotic.

For simulations, we have chosen $m_{11} = 0.1$ and $m_{33} = 0.1$ and parameter values $\alpha = 0.400$, $\beta = 0.175$, $\gamma = 0.400$ with initial conditions $(1, 1.5, 2.5)$. Then it can be observed that Fig.3 and Fig.4 show the phase portraits and calculated ellipsoidal surface. Hence all the state trajectories are found to remain within the predicted ellipsoidal surface. Also, we have selected $m_{11} = 0.1$, $m_{33} = 0.1$ and parameter values $\alpha = 0.100$, $\beta = 0.175$, $\gamma = 0.400$ with initial conditions $(1, 1.5, 2.5)$. Fig.5 shows the phase portraits and calculated ellipsoidal surface, and all state trajectories are found to remain into the predicted ellipsoidal surface. For same values of m_{11}, m_{33} and parameter values $\alpha = 0.400$, $\beta = 0.200$, and $\gamma = 0.400$ with initial conditions $(1, 1.5, 2.5)$, Fig.6 shows the phase portraits and calculated ellipsoidal surface, and again all the state trajectories are found to remain within the predicted ellipsoidal surface. For the synchronization purpose initial

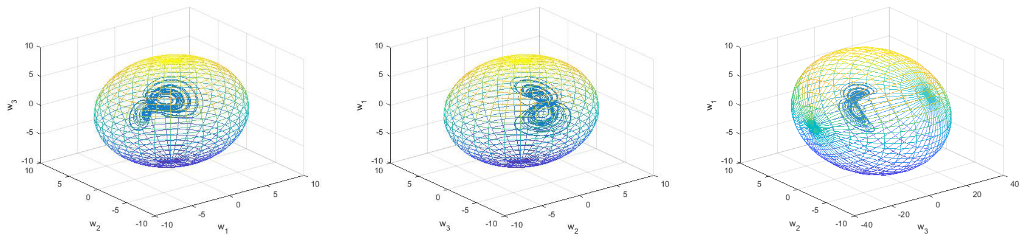

(A) (B) (C)

FIGURE 3. **(A)**, **(B)** , **(C)**: Phase portraits and ellipsoidal surface in 3D-space of the system (1) with $\alpha = 0.400$, $\beta = 0.175$, $\gamma = 0.400$, and $m_{11} = 0.1$, $m_{33} = 0.1$.

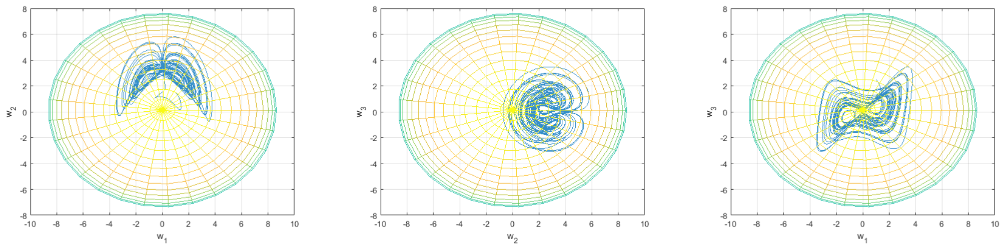

(A) (B) (C)

FIGURE 4. **(A)**, **(B)** , **(C)**: Phase portraits and elliptical curve in 2D-plane of the system (1) with $\alpha = 0.400$, $\beta = 0.175$, $\gamma = 0.400$, and $m_{11} = 0.1$, $m_{33} = 0.1$.

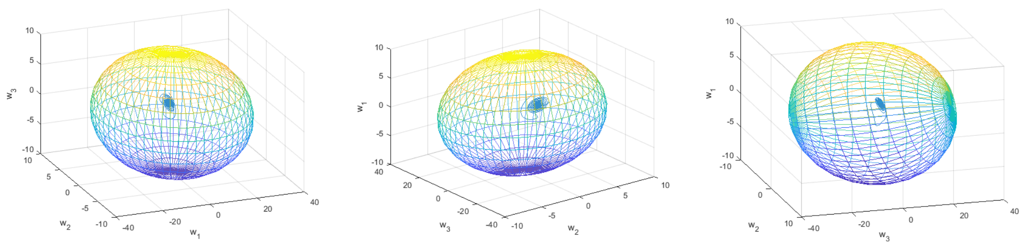

(A) (B) (C)

FIGURE 5. **(A)**, **(B)** , **(C)**: Phase portraits inside ellipsoidal surface in 3D-plane of the system (1) with $\alpha = 0.100$, $\beta = 0.175$, $\gamma = 0.400$, and $m_{11} = 0.1$, $m_{33} = 0.1$.

conditions of the master system (1) and slave system (30) are chosen as $(3, 5, -4)$ and $(-5, -2, 4)$, respectively. The controllers p_i, $i = 1, 2, 3$, are also defined by the coefficients $k_1 = 4$, $k_2 = 5$, and $k_3 = 16$. Hence, simulations show that the master and slave systems are synchronized and synchronization errors converge exponentially to zero, as illustrated in Fig.7.

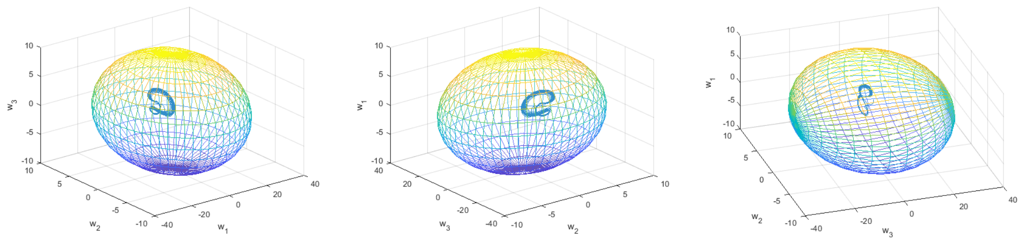

(A) (B) (C)

FIGURE 6. **(A)**, **(B)** , **(C)**: Phase portraits inside ellipsoidal surface in 3D-plane of the system (1) with $\alpha = 0.400$, $\beta = 0.200$, $\gamma = 0.400$, $m_{11} = 0.1$ and $m_{33} = 0.1$

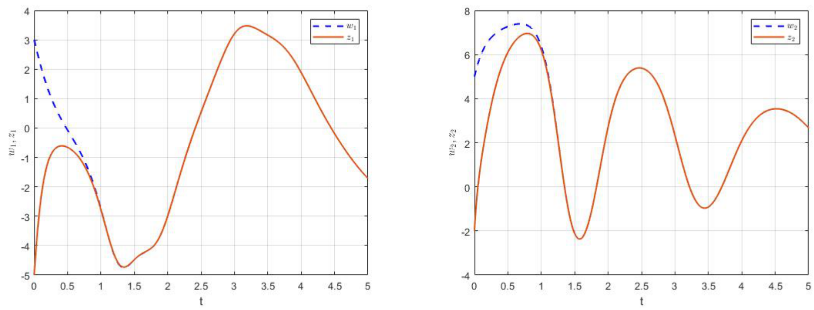

(A) (B)

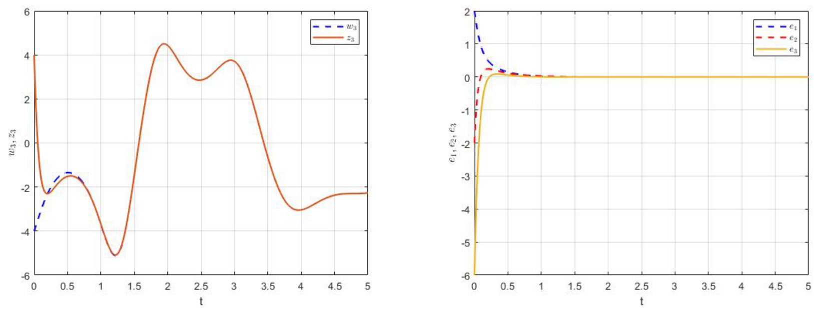

(C) (D)

FIGURE 7. (A), (B), (C) synchronized trajectories and (D) errors of chaotic systems (1) and (30).

6. A comparative analysis

In this section, we have provided a thorough comparative study between the existing works and the present work. In [36], authors proposed the predictive control stability and synchronization methodology of chaotic system and noticed that errors converge to zero at $t = 20(approx.)$ Adaptive synchronization for two identical satellite systems and observed that errors converge to zero at $t = 2.5(approx.)$ as studied in [37]. Further, Zadeh and Zadeh [38] have proposed synchronization scheme using active control method between two chaotic systems and noted that synchronized errors converge to zero at $t = 12(approx.)$. In [39], sliding mode control technique was applied to achieve synchronization between two identical chaotic systems and noticed that synchronize errors converge to zero at $t = 22(approx.)$. Whereas in presented work, the globally exponential synchronization technique is achieved using linear feedback control, and it is noticed that synchronization errors are converging to zero at $t = 1.5(approx.)$ as displayed in Fig.7. As the results

Table 1. Comparison between various results

Methods	Synchronization time(approx.)
Khan and Kumar [36]	$t = 20$
Khan and Kumar [37]	$t = 2.5$
Zadeh and Zadeh [38]	$t = 12$
Khan and Kumar [39]	$t = 22$
Present Method	$t = 1.5$

shown in the Table 1, one can observe that the synchronization time attained in our work is much less than all the aforementioned techniques.

7. Conclusion

The chaotic system is analysed in this work from the perspective of boundedness and synchronization. An ultimate bound sets (UBS) has been optimized for its ultimate bound which has been excellently used to analyse the solutions of the considered chaotic systems and then there qualitative and analytical nature has been deliberated. Bound set has been discussed for different parameter values. As an application of bound set, the linear feedback control method has been used to achieve globally exponential synchronization between two identical chaotic systems. The feasibility of the suggested method is shown by performing the simulations. These type of studies can be extended to investigate the boundary of the integer and fractional order chaotic and hyperchaotic systems.

Competing Interests Declaration

The authors do not have any competing interests or financial obligations from any organizations.

Acknowledgement

We are very thankful to all reviewers and editor office to enhance the quality and presentation of our research paper through their valuable suggestions and comments.

References

[1] Lorenz, E., (1963), Deterministic nonperiodic flow, Journal of Atmospheric Sciences, 20(2), pp. 130-141.

[2] Udaltsov, V. S., Goedgebuer, J. P., Larger, L., Cuenot, J. B., Levy, P., & Rhodes, W. T., (2003), Communicating with hyperchaos: the dynamics of a DNLF emitter and recovery of transmitted information, Optics and Spectroscopy, 95, pp. 114-118.

[3] Toker, D., Sommer, F. T., & D'Esposito, M., (2020), A simple method for detecting chaos in nature, Communications Biology, 3(1), pp. 11.

[4] Čenys, A., Tamaševičius, A., Baziliauskas, A., Krivickas, R., & Lindberg, E., (2003), Hyperchaos in coupled Colpitts oscillators, Chaos, Solitons & Fractals, 17(2-3), pp. 349-353.

[5] Yu, S., Lu, J., Yu, X., & Chen, G., (2012), Design and implementation of grid multiwing hyperchaotic Lorenz system family via switching control and constructing super-heteroclinic loops, IEEE Transactions on Circuits and Systems I: Regular Papers, 59(5), pp. 1015-1028.

[6] Wang, P., Zhang, Y., Tan, S., & Wan, L., (2013), Explicit ultimate bound sets of a new hyperchaotic system and its application in estimating the Hausdorff dimension, Nonlinear Dynamics, 74, pp. 133-142.

[7] Pogromsky, A. Y., Santoboni, G., & Nijmeijer, H., (2003), An ultimate bound on the trajectories of the Lorenz system and its applications, Nonlinearity, 16(5), pp. 1597.

[8] Leonov, G. A., Bunin, A. I., & Koksch, N., (1987), Attraktorlokalisierung des Lorenz-Systems, ZAMM-Journal of Applied Mathematics and Mechanics, 67(12), pp. 649-656.

[9] Leonov, G. A., & Kuznetsov, N. V., (2013), Hidden attractors in dynamical systems: From hidden oscillations in Hilbert–Kolmogorov, Aizerman, and Kalman problems to hidden chaotic attractor in Chua circuits, International Journal of Bifurcation and Chaos, 23(01), pp. 1330002.

[10] Li, Y., Wei, Z., & Aly, A. A., (2022), A 4D hyperchaotic Lorenz-type system: Zero-Hopf bifurcation, ultimate bound estimation, and its variable-order fractional network, The European Physical Journal Special Topics, 231(10), pp. 847-1858.

[11] Li, D., Wu, X., & Lu, J. A., (2009), Estimating the ultimate bound and positively invariant set for the hyperchaotic Lorenz–Haken system, Chaos, Solitons & Fractals, 39(3), pp. 1290-1296.

[12] Wang, P., Li, D., & Hu, Q., (2010), Bounds of the hyper-chaotic Lorenz–Stenflo system, Communications in Nonlinear Science and Numerical Simulation, 15(9), pp. 2514-2520.

[13] Nik, H. S., Effati, S., & Saberi, N. J., (2015), Ultimate bound sets of a hyperchaotic system and its application in chaos synchronization, Complexity, 20(4), pp. 30-44.

[14] Qin, W. X., (2007), On the boundedness of solutions of the Chen system, Journal of mathematical analysis and applications, 329(1), pp. 445-451.

[15] Zhang, F., Mu, C., & Li, X., (2012), On the boundness of some solutions of the Lü system, International Journal of Bifurcation and Chaos, 22(01), pp. 1250015.

[16] Lei, H., Li, T., Ma, Y., & Wang, H., (2018), Analyzing lattice networks through substructures, Applied Mathematics and Computation, 329, pp. 297-314.

[17] Zarei, A., & Tavakoli, S., (2016), Hopf bifurcation analysis and ultimate bound estimation of a new 4-D quadratic autonomous hyper-chaotic system, Applied Mathematics and Computation, 291, pp. 323-339.

[18] Wang, H., & Dong, G., (2019), New dynamics coined in a 4-D quadratic autonomous hyper-chaotic system, Applied Mathematics and Computation, 346, pp. 272-286.

[19] Wang, P., Li, D., Wu, X., Lü, J., & Yu, X., (2011), Ultimate bound estimation of a class of high dimensional quadratic autonomous dynamical systems, International Journal of Bifurcation and Chaos, 21(09), pp. 2679-2694.

[20] Mao, X., Feng, H., Al-Towailb, M. A., & Saberi N, H., (2023), Dynamical analysis and boundedness for a generalized chaotic Lorenz model, AIMS Mathematics, 8(8), pp. 19719-19742.

[21] Peng, Q., & Jian, J., (2021), Estimating the ultimate bounds and synchronization of fractional-order plasma chaotic systems, Chaos, Solitons & Fractals, 150, pp. 111072.

[22] Ren, L., Lin, M. H., Abdulwahab, A., Ma, J., & Saberi N. H., (2023), Global dynamical analysis of the integer and fractional 4D hyperchaotic Rabinovich system. Chaos, Solitons & Fractals, 169, pp. 113275.

[23] Jian, J., Wu, K., & Wang, B., (2020), Global Mittag-Leffler boundedness and synchronization for fractional-order chaotic systems, Physica A: Statistical Mechanics and its Applications, 540, pp. 123166.

[24] Ott, E., Grebogi, C., & Yorke, J. A., (1990), Erratum: 'Controlling chaos', Physical Review Letters, 64(23), pp. 2837.

[25] Carroll, T. L., & Pecora, L. M., (1995), Synchronizing chaotic circuits, Nonlinear dynamics in circuits, pp. 215-248.

[26] Rosenblum, M. G., Pikovsky, A. S., & Kurths, J., (1997), Phase synchronization in driven and coupled chaotic oscillators, IEEE Transactions on Circuits and Systems I: Fundamental Theory and Applications, 44(10), pp. 874-881.

[27] Khan, A., Nigar, U., & Chaudhary, H., (2022), Secure communication and synchronization dynamics in chaotic Chua's system via adaptive sliding mode control technique, International Journal of Applied and Computational Mathematics, 8(4), pp. 170.

[28] Harb, A. M., & Zohdy, M. A., (2009), Synchronization of two chaotic systems using nonlinear recursive controller, International Journal of Modelling and Simulation, 29(3), pp. 315-323.

[29] Khan, A., & Tyagi, A., (2017), Analysis and hyper-chaos control of a new 4-D hyper-chaotic system by using optimal and adaptive control design, International Journal of Dynamics and Control, 5, pp. 1147-1155.

[30] Laarem, G., (2021), A new 4-D hyper chaotic system generated from the 3-D Rösslor chaotic system, dynamical analysis, chaos stabilization via an optimized linear feedback control, it's fractional order

model and chaos synchronization using optimized fractional order sliding mode control, Chaos, Solitons & Fractals, 152, pp. 111437.
[31] Nijmeijer, H., (2001), A dynamical control view on synchronization, Physica D: Nonlinear Phenomena, 154(3-4), pp. 219-228.
[32] Sinha, S. C., Henrichs, J. T., & Ravindra, B., (2000), A general approach in the design of active controllers for nonlinear systems exhibiting chaos, International Journal of Bifurcation and Chaos, 10(01), pp. 165-178.
[33] Chien, F., Chowdhury, A. R., & Nik, H. S., (2021), Competitive modes and estimation of ultimate bound sets for a chaotic dynamical financial system, Nonlinear Dynamics, 106, pp. 3601-3614.
[34] Hu, X., & Nie, L., (2019), Exponential stability analysis of nonlinear systems with bounded gain error, Journal of Inequalities and Applications, 2019, pp. 1-8.
[35] Khan, A., & Kumar, S., (2018), Study of chaos in chaotic satellite systems, Pramana, 90, pp. 1-9.
[36] Khan, A., & Kumar, S., (2019), TS fuzzy modeling and predictive control and synchronization of chaotic satellite systems, International Journal of Modelling and Simulation, 39(3), pp 203-213.
[37] Khan, A., & Kumar, S., (2019), Measure of chaos and adaptive synchronization of chaotic satellite systems, International Journal of Dynamics and Control, 7, pp. 536-546.
[38] Ahmad, I., Saaban, A. B., Ibrahim, A. B., & Shahzad, M., (2015), Global chaos synchronization of new chaotic system using linear active control, Complexity, 21(1), pp. 379-386.
[39] Khan, A., & Kumar, S., (2018), Measuring chaos and synchronization of chaotic satellite systems using sliding mode control, Optimal Control Applications and Methods, 39(5), pp. 1597-1609.
[40] Ma, Y., Mou, J., Banerjee, S., Miao, M., (2023), A Quartic Nonlinear Flux-Controlled Memristor Model and its Application in Chaotic System, Appl. and Comput. Math., V. 3, p. 317

Prof. Ayub Khan has more than 30 years of teaching and research experience. Dr. Khan has published more than 150 research papers in various international and national academic Journals of repute. To his credit, he has successfully guided 23 Ph.D students. He is a regular reviewer of many national and international Journals. His research area is three-body problems, chaos synchronization and nonlinear dynamics.

Prof. Arshad Khan has more than 18 years of teaching and research experience. Dr. Khan has published more than 90 research papers in various international and national of repute. To his credit, he has successfully guided 9 Ph.D students. He is a regular national and international Journals. Dr Khan has been awarded DST project under Scheme for Young Scientist.

Mr. Shadab Ali is a PhD student in the department of Mathematics, Jamia Millia Islmia, New Delhi. His research interest is Qualitative Study of the Chaotic Systems and Chaos Synchronization. He has completed his master from IIT Ganhdinagar, Gujarat.